

δ -Ferrite Retention in the Weld Metal of P92 Heat-Resistant Steel Treated by CaF_2 - Cr_2O_3 Fluxes



HAOXIN LIU, MING ZHONG, YANYUN ZHANG, IMANTS KALDRE,
and CONG WANG

P92 heat-resistant steel has been successfully submerged arc welded by employing designed CaF_2 - Cr_2O_3 fluxes. It has been demonstrated that δ -ferrite is retained in the weld metal, the area fraction of which is found an approximately 3.7-fold enhancement as the Cr_2O_3 content in the fluxes is raised from 5 to 25 wt pct. Such phenomenon has been elucidated through governing element transfer behaviors incurred by the decomposition of Cr_2O_3 . Our findings possibly offer a viable solution towards developing welding fluxes geared towards durable heat-resistant steel grades.

<https://doi.org/10.1007/s11661-024-07420-w>

© The Minerals, Metals & Materials Society and ASM International 2024

I. INTRODUCTION

P92, a typical heat-resistant steel renowned for exceptional service temperature and high creep strength, has found extensive utilization as a preferred candidate for thermal power piping systems and nuclear power equipment.^[1] Submerged arc welding (SAW) with deep penetration and satisfactory weld quality has been practiced for manufacturing heat-resistant steels.^[2] However, high-temperature and high cooling rate of the weld pool render it inevitable that certain incomplete phase transformation products, such as δ -ferrite, could be retained in the weld metal (WM) after solidification. Wang *et al.*^[3] investigated phase transformation products of P91 steel and found that heterogeneous microstructures caused by retained δ -ferrite showed diverse crystallographic characteristics, especially on Kernel average misorientation (KAM) value. It is pointed out that retained δ -ferrite always demonstrates low KAM value compared with other products, potentially leading to deteriorated hardness, thereby invariably imposing adverse effects towards creep strength.^[4,5]

Generally, differing from the reheat zone in multi-pass welding, retained δ -ferrite content in the WM is largely dictated by the influence of major alloying element

contents, such as Cr, C, Mn, *etc.*^[6,7] The fraction of retained δ -ferrite could be enhanced by the increase of the Cr content.^[8] Alkan *et al.*^[9] changed Cr content in the 12Cr-Ni steel from 11.52 to 13.64 wt pct and the retained δ -ferrite fraction was found to experience appreciable enhancement from 5.5 to 33 pct. Meanwhile, Sam *et al.*^[10] and Arivazhagan *et al.*^[11] mentioned that the increase of C and Mn contents could reduce the amount of retained δ -ferrite in the WM microstructure. Wang *et al.*^[12] demonstrated that, for the 9Cr2WVTa steel, the accrual of C content from 0.08 to 0.16 wt pct was able to lower retained δ -ferrite from 6.7 to 3.5 pct. In addition, for Fe-21Cr-3Ni-1.7Mo-2.4C, varying Mn content from 0.4 to 2.4 wt pct incurred δ -ferrite fraction to decrease from 4 to 2.8 pct.^[13]

In SAW, a feasible approach achieving desirable WM composition and microstructure is to adjust welding fluxes.^[14,15] Under the effect of ultra-high temperatures, vehement chemical reactions could occur between flux (slag), molten pool, and arc, influencing the transfer of alloying elements.^[16-20] It is particularly worth mentioning that for P92 heat-resistant steel, Cr could serve as a solid solution strengthener and carbide former, and is regarded as the most important alloying element for heat-resistant steels. Low Cr content typically lead to coarsening of carbides and reduced mechanical properties. Generally, Cr in the WM is prone to loss through either evaporation or slag formation under high-temperature metallurgical reactions of SAW. Available studies have revealed that, by welding chromoly 4135 steel through SiO_2 - TiO_2 - CaO - MgO - Al_2O_3 - MnO - CaF_2 flux, Cr content decreased while O content increased in the WM.^[21] However, the addition of a Cr_2O_3 active agent-based SiO_2 - B_2O_3 - N_2O - Al_2O_3 flux in the welding process on 304 stainless steel enhanced Cr content in the WM.^[22] It is evident that the addition of

HAOXIN LIU, MING ZHONG, YANYUN ZHANG, and CONG WANG are with the Key Laboratory for Ecological Metallurgy of Multimetallic Mineral (Ministry of Education), Northeastern University, Shenyang 110819, P.R. China and also with the School of Metallurgy, Northeastern University, Shenyang 110819, P.R. China. Contact e-mail: wange@smm.neu.edu.cn IMANTS KALDRE is with the Institute of Physics, University of Latvia, Salaspils LV-2169, Latvia.

Manuscript submitted February 4, 2024; accepted April 16, 2024.

Cr₂O₃ in flux could effectively compensate for the lost Cr in the WM. However, illustrated effect of the Cr₂O₃ addition on the variations of other alloying elements, such as C and Mn, has not been fully documented. It is worth noting that current commercial fluxes are basically multicomponent, and it is difficult to single out the role of Cr₂O₃ oxide. Notably, existing research predominantly explores the regulation of composition in low-alloy steel through flux.^[16] However, there is a lack of studies on the impact of specific oxides in the flux on the WM for high-alloy steel.

In the present study, a simple while versatile CaF₂-Cr₂O₃ binary agglomerated flux system geared toward SAW has been designed for P92 heat-resistant steel. The variation of microstructure in the WM, especially retained δ -ferrite, has been investigated. Meanwhile, possible chemical reactions during welding have been postulated to elucidate element transfer behaviors between the fluxes and the WM.

II. EXPERIMENTAL PROCEDURE AND METHODS

Five CaF₂-Cr₂O₃ agglomerated fluxes were prepared, and the compositions of the fluxes are given in Table I. To match a suitable welding temperature and viscosity,^[23,24] Cr₂O₃ content was designed for 5, 10, 15, 20, and 25 wt pct, respectively, and CaF₂ was set to compensate for the rest. The fluxes were made from analytical reagent grade chemicals of CaF₂ (> 98.5 wt pct) and Cr₂O₃ (> 99.0 wt pct). After powders were mechanically mixed for 1 hour to ensure homogeneity, a sodium silicate binder whose weight is 20 pct relative to the weight of the mixed reagent was added for granulation into 10 to 50 mesh. The fluxes were then baked at 700 °C in air for 2 hours to improve particle strength and remove residual moisture of the fluxes. Bead-on-plate double-wires single-pass SAW (MZS-1250, Shangdong Aotai Electric, China) trials were performed on 25.4 mm thickness P92 heat-resistant steel. Thermanit MTS 616 was used as the welding wire. The welding speed was set as 500 mm/min, and a constant heat input of 60 kJ/cm (DC-850 A/32 V for electrode forward, AC-625 A/36 V for electrode backward) was employed.

Chemical compositions of base metal (BM), welding wire, and WM were determined. C and O were carried out by a LECO analyzer (ONH836, LECO Co.), and other elements were detected by an inductively coupled plasma optical emission spectrometry (ICP-OES, Optima 8300DV, Perkin Elmer). Compositions of BM, welding wire, and WM are summarized in Table II. For

convenience, corresponding WMs formed by the five prepared fluxes are designated as ‘WM1’, ‘WM2’, ‘WM3’, ‘WM4’, and ‘WM5’, representing the content of Cr₂O₃ in corresponding agglomerated flux for 5, 10, 15, 20, and 25 wt pct, respectively.

After welding, samples from the central region of the WM were cut, mechanically grounded, polished, and chemically etched by Vilella’s solution (1 g picric acid + 5 mL hydrochloric acid + 100 mL ethanol). Microstructures of the WMs were observed using a scanning electron microscope (SEM, MIRA3, TESCAN, Czech, acceleration voltage 20.0 kV). Crystallographic features were revealed by electron backscatter diffraction (EBSD, Nordlys Nano, Oxford Instruments, UK, operating voltage of 20.0 kV) system and HKL Channel5 software. The average δ -ferrite fraction of the WM area was determined through metallographic analysis. Specifically, after grinding, polishing, and etching each layer, over 30 fields measuring 0.5 × 0.5 mm² each were selected from SEM micrographs. The measurement was performed on at least three layers. Phase diagrams were calculated by FactSage 8.1 software using Fstel databases.^[25]

III. RESULTS AND DISCUSSION

Figure 1 illustrates the detailed room temperature microstructures in the WMs subjected to varied CaF₂-Cr₂O₃ fluxes. Generally, all WM microstructures demonstrate predominately martensite but with a small yet ineligible amount of δ -ferrite, which is distinguished by polygonal morphology and distributed randomly, as shown by the yellow dotted lines in Figures 1(a) through (e). In addition, the fraction of δ -ferrite increases with increasing Cr₂O₃ content in the fluxes. The quantitative relationship between the relative fraction of δ -ferrite and Cr₂O₃ content is shown in Figure 1(f). The result reveals that as the Cr₂O₃ content in the fluxes increases, there is a rise in the fraction of δ -ferrite in the WM, escalating from 1.87 ± 0.87 to 6.86 ± 1.49 pct. The variation represents an approximately 3.7-fold enhancement. The result is similar to the findings by Cai *et al.*^[26] Generally speaking, the phenomenon could be enabled by the synergistic effects of enhanced ferrite stabilizing elements (Cr, W, Mo, *et al.*) and reduced austenite stabilizers (C, Mn, *et al.*)^[27,28]

KAM maps of WMs, serving as the most intuitive indicators clearly distinguishing δ -ferrite and martensite, are shown in Figures 2(a) through (e). KAM maps are plotted based on the first neighbor kernel parameter with a maximum misorientation angle of 5 deg. KAM maps indicate that martensite laths show high KAM values while δ -ferrites possess low KAM values (almost 0 deg).^[29,30] From WM1 to WM5, it can be seen that the blue area, about 0 deg KAM, gradually reduces. Statistic results of KAM distributions in the selective area are shown in Figure 2(f), and the average KAM values of WM1 to WM5 are 1.46, 1.42, 1.36, 1.35, and 1.30, respectively. It is well-known that higher misorientation angles indicate increased dislocation density and higher degree of strain localization.^[31] With the increase of

Table I. Chemical Compositions of Employed Fluxes (Weight Pct)

	Flux-1	Flux-2	Flux-3	Flux-4	Flux-5
Cr ₂ O ₃	5	10	15	20	25
CaF ₂	90	85	80	75	70

Table II. Chemical Compositions of Base Metal, Welding Wire and Weld Metal (Weight Pct)

	C	Si	Mn	Cr	Mo	W	N	V	Nb	Ni	O
Base Metal	0.097	0.242	0.396	8.902	0.430	1.731	0.046	0.208	0.011	0.234	0.002
Welding Wire	0.102	0.270	0.772	8.624	0.440	1.915	0.046	0.184	0.051	0.440	0.002
WM1	0.091	0.264	0.394	9.121	0.466	1.860	0.043	0.195	0.021	0.311	0.043
WM2	0.090	0.192	0.379	9.483	0.449	1.840	0.043	0.195	0.021	0.307	0.070
WM3	0.089	0.150	0.301	9.739	0.453	1.830	0.043	0.194	0.018	0.275	0.082
WM4	0.088	0.107	0.278	9.851	0.451	1.820	0.042	0.194	0.017	0.258	0.100
WM5	0.087	0.080	0.254	9.868	0.450	1.820	0.042	0.194	0.016	0.237	0.105

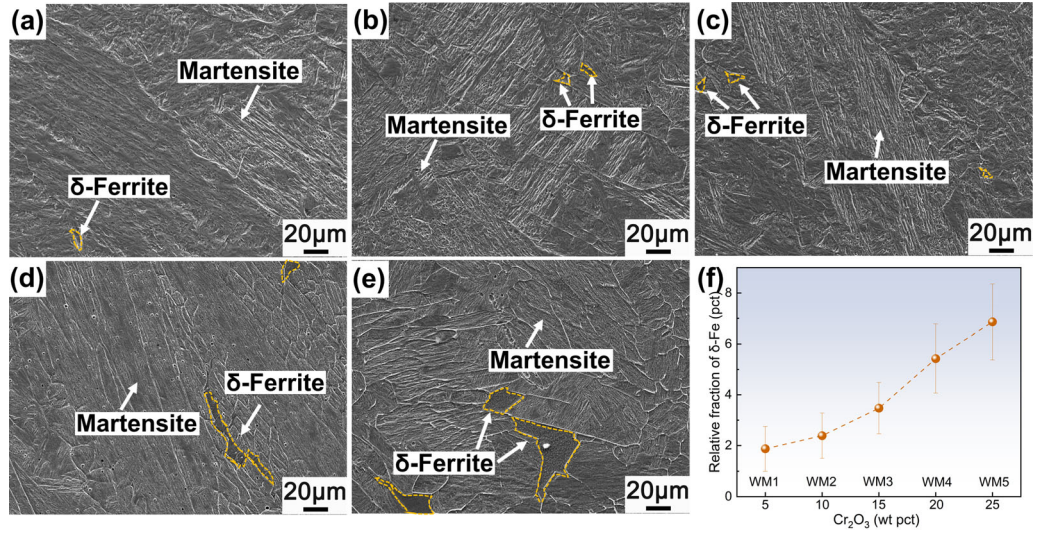


Fig. 1—Typical microstructures of: (a) WM1, (b) WM2, (c) WM3, (d) WM4, and (e) WM5; (f) relative fraction of δ -ferrite in the weld metal as a function of Cr_2O_3 (Color figure online).

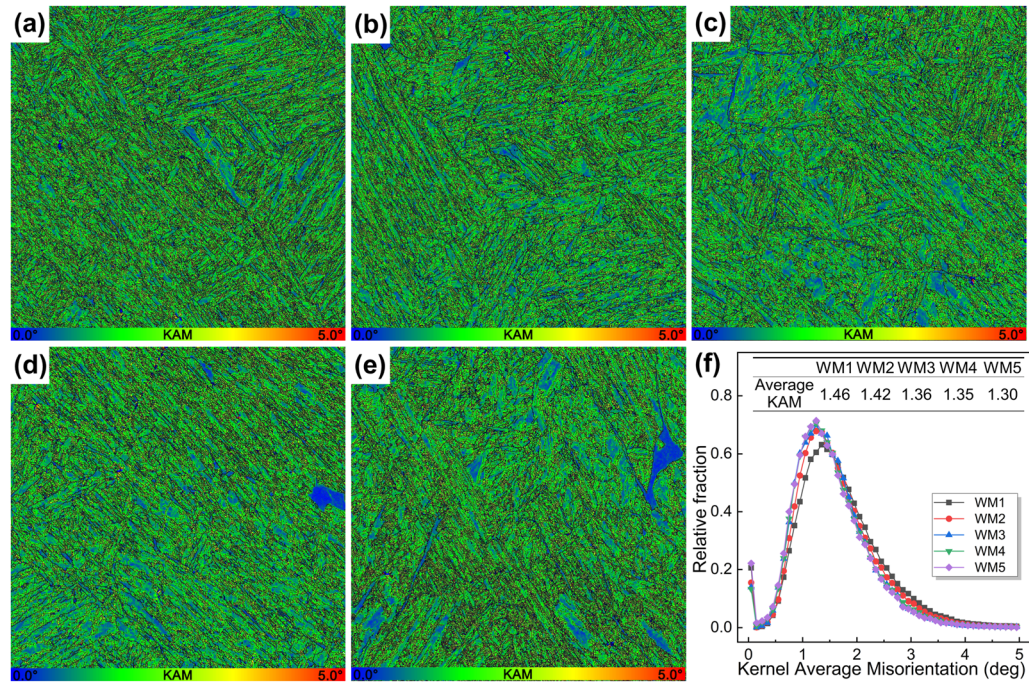


Fig. 2—Kernel average misorientation map of WMs: (a) WM1, (b) WM2, (c) WM3, (d) WM4, (e) WM5, and (f) KAM distribution (Color figure online).

δ -ferrite, the average KAM value displays a depreciated density of dislocations, imparting lower resistance that must be overcome during plastic deformation.^[32]

δ -Ferrite retention is closely related to alloying elements in WMs, which can be estimated by empirical formulas.^[3,10] Generally, when the ferrite factor (FF), that is, the difference between the chromium equivalent (Cr_{eq}) and the nickel equivalent (Ni_{eq}), is less than 10, no ferrite could exist in the microstructure. Cr_{eq} and Ni_{eq} are given by the Newhouse formula,^[33] as displayed in Eqs. [1] and [2]:

$$Cr_{eq} = Cr + 6Si + 4Mo + 11V + 5Nb + 1.5W + 12Al + 8Ti \quad [1]$$

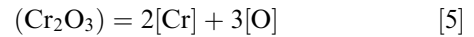
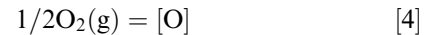
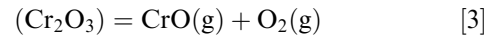
$$Ni_{eq} = 2Mn + 4Ni + 40C + 30N + 2Co + Cu \quad [2]$$

where components are in weight percentages. Table III shows the calculated results from the chemical composition of the WMs according to analyzed chemical compositions (Table II). It can be seen that all FF values are more than 10, implying retained δ -ferrite could be present for all WMs.

Figure 3 shows WM phase diagrams calculated by the FactSage 8.1 software. Calculated results show that the δ -ferrite phase region expands while the γ -austenite phase region shrinks with the addition of Cr_2O_3 in the fluxes, as displayed in the black (WM1) and purple (WM5) stars in Figure 3. It is further shown that the transformation temperature of $\delta \rightarrow \gamma$ is lowered, while that of $\gamma \rightarrow$ martensite is increased, meaning the dwell time at $\delta + \gamma$ and γ phase fields is shortened during the cooling process.^[34] Previous studies have demonstrated that retained δ -ferrite is enabled by the incomplete $\delta \rightarrow \gamma$ phase transformation.^[35] The shorter the time spent in the $\delta + \gamma$ and γ phase fields, the higher the content of the δ -ferrite retained in the microstructure.^[10] The aforementioned phenomenon may be caused by the variation of ferrite or austenite stabilizing elements.^[36] Both the increase of ferrite stabilizer (Cr) and the decrease of austenite stabilizing element (Mn or C) could reduce the diffusion coefficient of C atoms, which may possibly delay the austenite transformation (as shown by the points A to C in Figure 3).^[37,38] In addition, the reduction of C content increases supercooling of martensite transformation, thus the austenite to martensite transformation temperature is enhanced, as displayed the points B to D in Figure 3.^[39]

It is well-known variation of alloying elements in the WM could be incurred by metallurgical reactions.^[40] In SAW, Cr_2O_3 in the fluxes could decompose and release

O_2 under the influence of high-temperature plasma of the welding arc in the arc cavity (Eq. [3]). Oxides in the flux provide the total source of O for SAW WM due to flux preventive effect on oxidization by the atmosphere.^[41] O_2 in the arc cavity could supply O from the fluxes to the WM through gas-metal reactions occurring at the gas-slag interface (Eq. [4]),^[41] enhancing O content in the WM. Further, a previous study has shown the negative Gibbs free energy (ΔG) of Cr_2O_3 decomposition reaction (Eq. [5]), indicating that the main source of Cr in the WM is the decomposition of Cr_2O_3 rather than the transition of suboxide (CrO). Cr_2O_3 reacting at the slag-metal interface and transferring Cr and O from the flux into the WM.^[42] As the addition of Cr_2O_3 in flux increases from 5 to 25 wt pct, the activity of Cr_2O_3 increases from 0.447 to 0.557, while ΔG values vary from -160.47 to -62.17 kJ/mol (calculated by FactSage 8.1), indicating a reduced driving force of Cr_2O_3 decomposition. Thus, contents of Cr and O in the WM are enhanced, which vary from 0.043 to 0.105 wt pct and 9.121 to 9.868 wt pct, respectively, as shown in Table II.



Furthermore, O in the weld pool could react with certain alloying elements at the slag-metal or gas-metal interface to form oxides, resulting in the loss of alloying elements in the WM.^[16,41] Mn can combine with O in the weld pool and transfer to the slag in the form of MnO through slag-metal reactions, as shown in Eq. [6]. With the addition of Cr_2O_3 content, O content in the WM enhanced, which may significantly increase the driving force for Eq. [6]. Therefore, with the Cr_2O_3 varying from 5 to 25 wt pct, Mn content decreases from

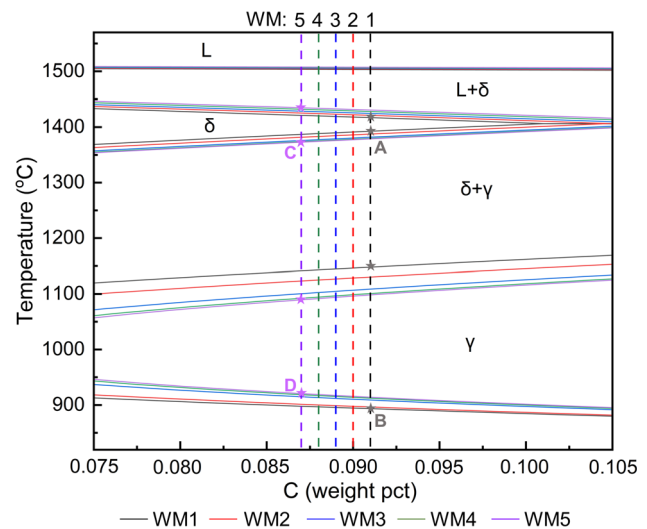
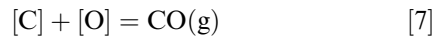
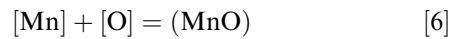


Fig. 3—WM equilibrium phase diagrams (Color figure online).

Table III. Ferrite Factor of WMs Predicted by the Empirical Formula

	WM1	WM2	WM3	WM4	WM5
Cr_{eq}	17.61	17.44	17.42	17.25	17.09
Ni_{eq}	7.02	6.87	6.55	6.37	6.20
Ferrite Factor	10.65	10.57	10.87	10.88	10.89

0.394 to 0.254 wt pct in the WM. Similarly, Si loses from the WM to the slag in the form of Si-oxide through slag-metal reactions.^[43] C loses from the WM and transitions into the arc cavity in the form of CO, as shown in Eq. [7].^[43] In addition, it needs to be mentioned that the reduction in Ni concentration within the WM is attributed to two primary factors: (1) a decline in Ni content with the escalating dilution of the WM,^[44] and (2) the transfer of Ni from the WM to the slag.^[45]



IV. CONCLUSIONS

In summary, the present study illustrates a variation of retained δ -ferrite in the WMs of P92 heat-resistant steel as a function of Cr_2O_3 in $\text{CaF}_2\text{-Cr}_2\text{O}_3$ flux, and the phenomena are elucidated *via* salient chemical reactions. The main conclusions are as follows:

1. The microstructure of WM is composed of martensite and retained δ -ferrite. As the content of Cr_2O_3 in the fluxes improves from 5 to 25 wt pct, the retained δ -ferrite content increases from 1.87 ± 0.87 to 6.86 ± 1.49 pct, and corresponding average KAM values reduce from 1.46 to 1.30.
2. When the addition of Cr_2O_3 in the fluxes increases, a series of metallurgical reactions in the weld pool occurs, enhancing Cr content while decreasing the contents of Mn, C, and Ni in the WMs, leading to appreciable increase of retained δ -ferrite fraction.

ACKNOWLEDGMENTS

The authors wish to thank the financial support from the National Key Research and Development Program of China [Grant Nos. 2022YFE0123300 and 2023YFB3709900], National Natural Science Foundation of China [Grant Nos. U20A20277 and 52350610266].

CONFLICT OF INTEREST

On behalf of all authors, the corresponding author states that there is no conflict of interest.

REFERENCES

1. K.M. Chalk, P.H. Shipway, and D.J. Allen: *Sci. Technol. Weld. Join.*, 2011, vol. 16, pp. 613–18.
2. U.K. Mohanty, Y. Abe, T. Fujimoto, M. Nakatani, A. Kitagawa, M. Tanaka, T. Suga, and A. Sharma: *J. Press. Vessel*, 2020, vol. 142, p. 041506.
3. Y. Wang, R. Kannan, L. Zhang, and L. Li: *Weld. J.*, 2017, vol. 96, pp. 203–19.

4. Y. Shen, Z. Gu, and C. Wang: *Acta Metall. Sin.*, 2023, <https://doi.org/10.11900/0412.1961.2023.00045>.
5. D. Wu, W. Tian, K. Zhang, and S. Lu: *Sci. Technol. Weld. Join.*, 2023, vol. 28, pp. 242–48.
6. S.S. Mahlalela and P.G.H. Pistorius: *Weld. World.*, 2023, vol. 67, pp. 1169–80.
7. S.G. Park, M.C. Kim, B.S. Lee, and D.M. Wee: *J. Nucl. Mater.*, 2010, vol. 407, pp. 126–35.
8. B. Zhang, H. Wang, X. Ran, X. Nie, J. Wang, and B. He: *Mater. Charact.*, 2022, vol. 190, p. 112080.
9. G. Alkan, D. Chae, and S.J. Kim: *Mater. Sci. Eng. A*, 2013, vol. 585, pp. 39–46.
10. S. Sam, C.R. Das, V. Ramasubbu, S.K. Albert, A.K. Bhaduri, T. Jayakumar, and E. Rajendra Kumar: *J. Nucl. Mater.*, 2014, vol. 455, pp. 343–48.
11. B. Arivazhagan, M. Vasudevan, and M. Kamaraj: *Met. Mater. Int.*, 2015, vol. 21, pp. 538–42.
12. J. Wang, L. Rong, D. Li, and S. Lu: *J. Nucl. Mater.*, 2017, vol. 485, pp. 169–80.
13. M.J. Kadhim, A.N. Abood, and R.S. Yaseen: *Mod. Appl. Sci.*, 2011, vol. 5, p. 179.
14. M. Zhong, D. Guo, S. Basu, Z. Wang, and C. Wang: *J. Iron. Steel Res. Int.*, 2023, vol. 30, pp. 569–79.
15. Y. Zhang, H. Yuan, H. Tian, Z. Wang, and C. Wang: *Metall. Mater. Trans. B*, 2023, vol. 54, pp. 3023–30.
16. C. Wang and J. Zhang: *Acta Metall. Sin.*, 2021, vol. 57, pp. 1126–40.
17. K. Bang, C. Park, H. Jung, and J. Lee: *Met. Mater. Int.*, 2009, vol. 15, pp. 471–77.
18. Y. Wu, X. Yuan, I. Kaldre, M. Zhong, Z. Wang, and C. Wang: *Metall. Mater. Trans. B*, 2023, vol. 54B, pp. 50–55.
19. I. Kaldre, M. Zhong, Y.W. Wu, and C. Wang: *Mater. Sci. Forum*, 2023, vol. 1095, pp. 133–38.
20. X. Yuan, Y. Wu, M. Zhong, S. Basu, Z. Wang, and C. Wang: *Sci. Technol. Weld. Join.*, 2022, vol. 27, pp. 683–90.
21. M. Alishavandi, M. Mohammadmirzaei, M. Ebadi, and A.H. Kokabi: *J. Mater. Process. Technol.*, 2021, vol. 290, p. 116890.
22. L. Mei, D. Yan, S. Xie, Z. Lei, and X. Ge: *Opt. Lasers Eng.*, 2020, vol. 128, p. 106027.
23. C.A. Natalie, D.L. Olson, and M. Blander: *Annu. Rev. Mater. Sci.*, 1986, vol. 16, pp. 389–413.
24. Z. Wang, Z. Li, M. Zhong, Z. Li, and C. Wang: *J. Non-Cryst. Solids*, 2023, vol. 601, p. 122071.
25. I.H. Jung and M.A. Van Ende: *Metall. Mater. Trans. B*, 2020, vol. 51B, pp. 1851–74.
26. Y. Cai, Z. Luo, and Y. Zeng: *Sci. Technol. Weld. Join.*, 2017, vol. 22, pp. 236–43.
27. P. Mayr, T.A. Palmer, J.W. Elmer, E.D. Specht, and S.M. Allen: *Metall. Mater. Trans. A*, 2010, vol. 41A, pp. 2462–65.
28. M.W. Kuper and B.T. Alexandrov: *Metall. Mater. Trans. A*, 2019, vol. 50A, pp. 2732–47.
29. Y. Wang and L. Li: *Weld. J.*, 2016, vol. 95, pp. 27–36.
30. A. Khajuria, M. Akhtar, R. Bedi, R. Kumar, M. Ghosh, C.R. Das, and S.K. Albert: *Mater. Sci. Technol.*, 2020, vol. 36, pp. 1407–18.
31. J. Li, H. Li, Y. Liang, P. Liu, and L. Yang: *Materials*, 2019, vol. 12, pp. 1–15.
32. X. Di, D. Geng, S. Wu, D. Wang, Z. Zhang, and C. Li: *Sci. Technol. Weld. Join.*, 2019, vol. 24, pp. 148–55.
33. S.S. Mahlalela and P.G.H. Pistorius: *Weld. World.*, 2022, vol. 66, pp. 1191–98.
34. Y. Zhang, D. Zou, X. Wang, Y. Li, M. Li, F. Wang, W. Zhang, and L. Tong: *J. Mater. Res. Technol.*, 2022, vol. 18, pp. 3104–14.
35. H. Liu, M. Zhong, Y. Shen, Z. Wang, S. Basu, and C. Wang: *Mater. Charact.*, 2023, vol. 200, p. 112864.
36. S.M.K. Hosseini, A. Zarei Hanzaki, and S. Yue: *Mater. Sci. Eng. A*, 2015, vol. 626, pp. 229–36.
37. N. Saini, R.S. Mulik, M.M. Mahapatra, and L. Li: *Metall. Mater. Trans. B*, 2023, vol. 54B, pp. 315–30.
38. O.K. Rowan and R.D. Sisson: *J. Phase Equilib. Diff.*, 2009, vol. 30, pp. 235–41.
39. H. Zou, H. Hu, G. Xu, Z. Xiong, and F. Dai: *Metals*, 2019, vol. 9, p. 138.
40. M. Zhong, T. Li, S. Basu, Z. Wang, and C. Wang: *Metall. Mater. Trans. B*, 2022, vol. 53B, pp. 2774–78.

41. Y. Zhang, J. Zhang, H. Liu, Z. Wang, and C. Wang: *Metall. Mater. Trans. B*, 2022, vol. 53B, pp. 1329–34.
42. H. Liu, Y. Zhang, M. Zhong, Y. Feng, J. Liu, and C. Wang: *Metall. Mater. Trans. B*, 2024, vol. 55B, pp. 8–13.
43. U. Mitra and T.W. Eagar: *Metall. Trans. A*, 1984, vol. 15A, pp. 217–27.
44. B. Singh, Z.A. Khan, A.N. Siddiquee, and S. Maheshwari: *Sādhanā*, 2018, vol. 43, p. 26.
45. B.R. Vishnu, S.P. Sivapirakasam, K.K. Satpathy, S.K. Albert, and G. Chakraborty: *J. Manuf. Process.*, 2018, vol. 34, pp. 713–20.

Publisher's Note Springer Nature remains neutral with regard to jurisdictional claims in published maps and institutional affiliations.

Springer Nature or its licensor (e.g. a society or other partner) holds exclusive rights to this article under a publishing agreement with the author(s) or other rightsholder(s); author self-archiving of the accepted manuscript version of this article is solely governed by the terms of such publishing agreement and applicable law.